

STUDY OF CHANNELING AND VOLUME REFLECTION EFFECTS IN BENT CRYSTALS

PNPI participants of the Russia-Italy-USA-CERN Collaboration:

Yu.M. Ivanov, N.F. Bondar, Yu.A. Gavrikov, A.S. Denisov, A.V. Zhelamkov, V.G. Ivochkin, S.V. Kosyanenko, L.P. Lapina, A.A. Petrunin, V.V. Skorobogatov, V.M. Suvorov, A.I. Shchetkovsky

1. Introduction

In the last years it has been shown that short bent silicon crystals can be used efficiently to extract beam particles out of the accelerators. This crystal extraction was applied to the main beam and also to the halo particles. The idea of crystal based collimation for the Large Hadron Collider (LHC) at CERN is to use bent crystals for deflecting the halo protons at 6σ from the central beam orbit onto a special absorber where they hit with large impact parameters. Due to large deflection angles and high impact parameters the halo protons can be efficiently removed using crystals from the LHC beams that should reduce background in detectors and avoid quenches of superconducting magnets at highest luminosities. Below we describe our recent studies of silicon properties and beam-crystal interactions performed at PNPI, IHEP, and CERN with the aim to develop high efficient crystal collimation system for the LHC.

2. Observation of elastic quasi-mosaicity effect in silicon

Multiple scattering of high energy charged particles in material restricts an efficiency of the crystals as beam deflectors. Estimations show that optimal size of the bent silicon crystals in beam direction should lie in millimeter or sub-millimeter region with the bending angles of the atomic planes not exceeding one-two hundred microradians. We found that such requirements can be met using elastic quasi-mosaicity effect in bent silicon plates.

This effect is well-known in crystal-diffraction γ - and X -rays spectrometry after studies carried out by O.I. Sumbaev in 60-es. He showed that bending of quartz plate results in the curving of atomic planes coinciding with normal cross sections of the plate. It broadens the diffraction profiles of γ -lines as if the plate was the mosaic crystal. In 70-es, A.V. Tyunis, V.M. Samsonov and O.I. Sumbaev generalized the theory of the effect and predicted that some other materials (*i.e.* silicon) should reveal elastic quasi-mosaicity behavior.

We investigated with X -rays the properties of silicon plates cut under different angles with respect to the crystallographic axes and observed the elastic quasi-mosaicity effect for the (111) atomic planes [1]. The plate orientation respect to the crystallographic planes corresponding to the largest elastic quasi-mosaicity effect in silicon is shown in Fig. 1.

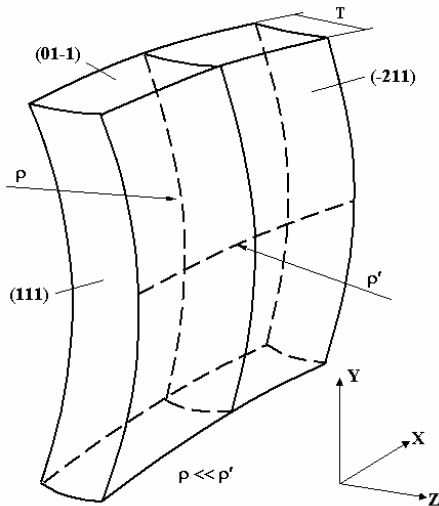


Fig. 1. Elastic quasi-mosaicity effect in bent silicon plate: the bending of the plate to a cylinder of radius ρ results in curving of the (111) crystallographic planes along thickness T . The radius ρ' characterizes the curvature induced by anticlasic forces

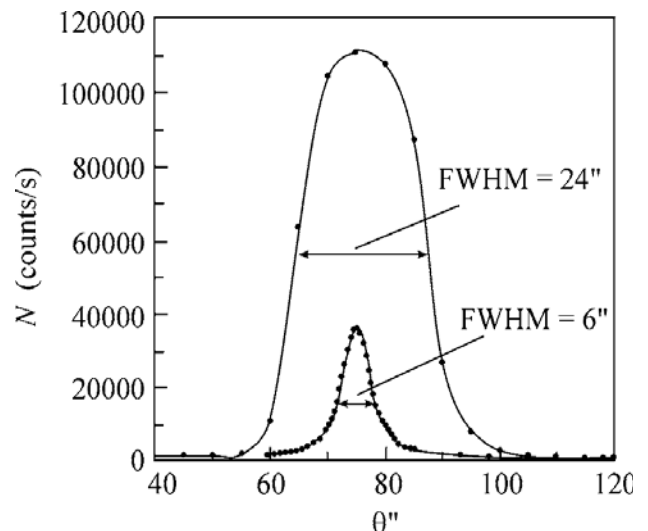


Fig. 2. Rocking curves before and after bending of the sample (FWHMs are 6" and 24", respectively)

Using double crystal X-rays diffractometer in the transmission mode we measured rocking curves of the sample with sizes $20(X) \times 60(Y) \times 0.43(Z)$ mm³ before and after bending. The measurement results are shown in Fig. 2, where both rocking curves are presented. The FWHM of the rocking curve for unbent plate is equal to $6''$ and close to the width from two ideal crystals. After the bending of the sample to a radius of $\rho = 92$ cm in vertical plane, the rocking curve width and amplitude increase by a factor of 4. The width of the rocking curve directly characterizes a bending angle of the (111) atomic planes along plate thickness. It is equal to $24''$ that means bending angle $120 \mu\text{rad}$ per 0.43 mm. Due to anticlastic forces a shape of the bent plate is similar to the “saddle” with a radius of $\rho' = 410$ cm in the horizontal plane.

The control experiment was made with another plate cut from the same ingot. This plate was identical to the studied above but differed in the cut angle in the (111) plane by 30° . After the bending of the control plate, its rocking curve practically did not change.

The measured bending angles of atomic planes in silicon were found to be in a good agreement with the updated theory predictions and close to values needed for crystal collimation.

3. Observation of volume reflection effect in bent silicon crystal with 70 GeV proton beam at IHEP

Using elastic quasi-mosaicity effect in silicon we prepared a series of bent crystals with sub-millimeter lengths along beam and studied them at the Institute for High Energy Physics (Protvino) with 70 GeV protons. In the experiment, besides channeling, we observed a volume reflection of protons in the bent crystal [2, 3], the new effect essential for development of crystal applications at accelerators predicted by A.M. Taratin and S.I. Vorobiev in 80-es. This phenomenon arises from the coherent interaction of proton with a bent atomic plane in the tangency point of the plane with the proton trajectory and results in a small angular deflection of the reflected particle opposite the atomic plane bending.

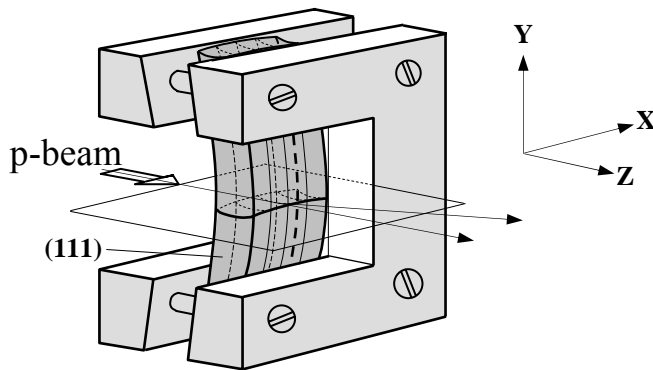


Fig. 3. Bending method of Si (111) planes (coinciding with vertical narrow face of crystal plate)

Silicon plate used in experiment had sizes $20(X) \times 60(Y) \times 0.72(Z)$ mm³ with channeling (111) planes parallel to the YZ plane. The plate was bent in the YZ plane using method of applied moments (Fig. 3) to a radius of 48 cm that induced a quasi-mosaic bending of the (111) planes in the XZ plane to a radius of 1.7 m with a full bending angle of $\sim 420 \mu\text{rad}$. The saddle radius in the XZ plane was found to be about 3.2 m in the center of the crystal with increasing to the clamping areas.

The crystal was mounted on a turntable providing 4 mm overlapping with the proton beam in the X-direction (Fig. 4). Alignment of the crystal was done using a reflection of laser beam from crystal faces to the marks related with proton beam. Channeling orientation of the crystal was found as an angular position with maximal coincidence rate between narrow scintillation counters S1 and S2 placed in and out of the primary beam, respectively. A large counter S3 was used as a primary beam monitor.

The crystal was mounted on a turntable providing 4 mm overlapping with the proton beam in the X-direction (Fig. 4). Alignment of

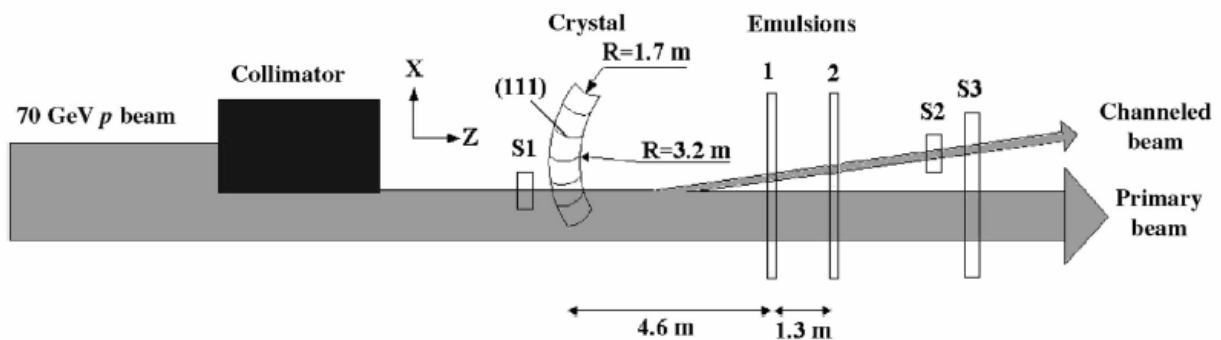


Fig. 4. Layout of the experiment. S1, S2, S3 – scintillation counters

In the experiment we used a small-divergent ($\sim 15 \mu\text{rad}$), low intensity ($\sim 10^5 \text{ s}^{-1}$), external 70 GeV proton beam. The angular spreading of the beam induced by the multiple scattering in the crystal plate was $13.5 \mu\text{rad}$. Both the divergence of the incident beam and the multiple scattering in the crystal were small with respect to the critical angle for channeling θ_c equal to $24 \mu\text{rad}$ in our case.

The profile of the beam transmitted through the oriented crystal was measured using emulsions of the R-100 type located 4.6 m and 5.9 m downstream. They were exposed to an integrated flux of about 5 particles/ $(\mu\text{m})^2$ and displayed three slightly distinct curved lines A, B, and C. The lines were well visible in a wide background spot from primary beam having a semicircle shape due to cutting a beam by collimator. The measured profiles were similar in both emulsions, but separation of lines was largest in the most distant emulsion, which is shown in Fig. 5. For both emulsions we determined the relative positions and widths of the observed lines in the X-direction of the crystal mid-plane with a microscope (along the white dashed line in Fig. 5).

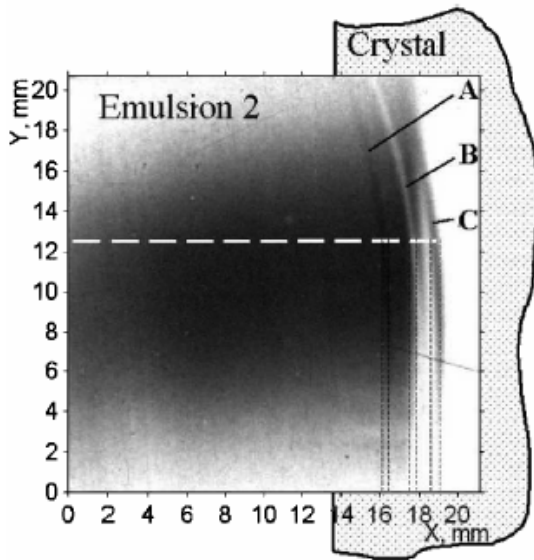


Fig. 5. Part of emulsion 2 with the profile of the proton beam. The white dashed line indicates the trace of the measurement with a microscope. The black dashed lines show X-readings, which correspond to the borders of the lines A, B, and C

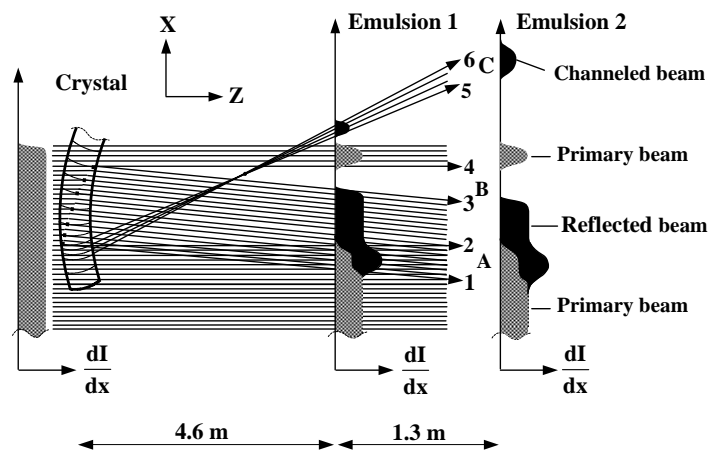


Fig. 6. Proton trajectories crossing the crystal and emulsions in the horizontal plane (top view). The incident beam is shown as parallel (distance between the effective “source” of the beam and the crystal is much larger than a saddle radius of the crystal) with a uniform intensity distribution along the X-direction. The dots within the crystal indicate the tangency points of the incident proton trajectories with the (111) atomic planes where the volume reflection takes place

An explanation of the beam intensity distribution observed in emulsions is given in Fig. 6 where proton trajectories in the horizontal XZ-plane are shown. The crystal has curvature in this plane due to anticlasic forces so the (111) planes change orientation along the X-direction. In a small X-range, where incident protons are tangent to the (111) planes on the entry face, part of the protons transiting through this range are captured in the channeling along the (111) planes (rays between 5 and 6) producing a spot C. For points at larger X-coordinates, the conditions are adequate for volume reflection, since the trajectories of the incident protons are tangent to the atomic (111) planes somewhere inside the crystal (rays in between 1 and 3). Out of the X-ranges for the channeling and volume reflection, incident protons pass through the crystal and experience only multiple scattering (rays above ray 4 and below 2). In this case, there is an area depleted of protons in between the reflected and primary beams, denoted by B, and another area where primary and reflected protons mix, denoted by A.

Above or below the mid-plane, we have the same picture of the proton-crystal interactions, except that the vertical dependence of the anticlasic curvature produces a continuous shifting of the projected spots. As result, a joint pattern comprises three lines (two black lines A and C and one light line B) of the same slightly curved shape.

The deflection angle of the channeled protons is estimated from the ratio of the distance between lines A and C to the distance between the crystal and the corresponding emulsion. Averaging over two emulsions, we found a value of $435 \pm 6 \mu\text{rad}$ that coincides with the bending angle of the (111) planes measured with X-rays.

The deflection angle $2\theta_r$ of the reflected protons is estimated from the angular width of lines A and B, defined as the ratio of the line width to the distance from the crystal to each emulsion. Averaging the widths of A and B, we found $2\theta_r$ equal to $39.5 \pm 2.0 \mu\text{rad}$, or $(1.65 \pm 0.08) \cdot \theta_c$ in terms of the critical angle for channeling.

The dark color of the line A shows that probability of the reflection is larger than probability of the channeling. The widths of the reflected and channeled beams demonstrate that an angular acceptance of the volume reflection determined by a bend angle of the atomic planes is larger than an angular acceptance of the channeling restricted by a critical angle θ_c .

4. Study of volume reflection effect in bent silicon crystals with 1 GeV proton beam at PNPI

In the experiment with emulsion detectors, only a qualitative estimate for the reflection probability was obtained. In the next experiment with the use of electronic detectors the channeling and reflection effects were registered separately providing accurate estimates for the probabilities of the processes [4, 5].

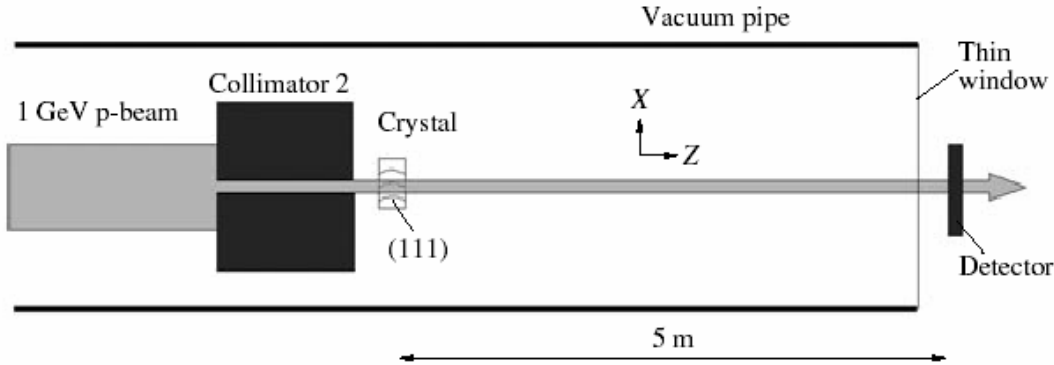


Fig. 7. Layout of the experiment on the observation of volume reflection with the 1 GeV proton beam

This experiment was carried out at the 1 GeV proton synchrocyclotron. The method (Fig. 7) involved the formation of a narrow, almost parallel, proton beam incident on a crystal and measurement of the distribution of the protons deflected by the crystal using fast-response detectors with high position resolution.

The beam was formed by means of two collimators near 1 m in length and separated by a distance of 31 m from one to another with a deflecting magnet between them. The adjusted proton beam had half-width in the horizontal plane at the exit of the second collimator equal to $80 \pm 20 \mu\text{m}$ with the angular divergence of $160 \pm 20 \mu\text{rad}$ and intensity of about 2×10^4 protons per second.

A silicon plate similar to the shown in Fig. 1 was used as the working crystal. The thickness of the plate was $30 \mu\text{m}$ that corresponds to the multiple scattering angle of $105 \mu\text{rad}$ (smaller than a critical angle for channeling equal to $170 \mu\text{rad}$ for the (111) silicon planes and 1 GeV protons). The plate was bent with a radius of 22 mm in the vertical plane by means of clamping in cylindrical mirrors with a hole with a diameter of 3 mm at the center for passing the proton beam. The quasi-mosaic bending of the (111) planes measured with X-rays was found to be $380 \pm 20 \mu\text{rad}$. The bent crystal was mounted on the rotary table attached to the exit end of the second collimator so that the center of the crystal coincided with the proton beam axis. Position-sensitive detectors were placed at a distance of 5 m from the crystal outside the vacuum channel.

One of the detectors was a parallel plate gas counter with linear position sensitivity (due to dividing anode plane into 64 elements with $200 \mu\text{m}$ pitch), the other was a cross of two scintillation counters (with $80 \mu\text{m}$ widths) placed on a linear carriage and working in coincidence. The both detectors had detection area for protons limited in the vertical direction and allowed measurements of the beam profile in the horizontal plane.

Figure 8 shows the typical angular scan with the parallel plate counter. The X-axis is the anode-strip coordinate in millimeters, zero corresponds to the position of the primary beam axis. The θ -axis is the

crystal angle in microradians, zero corresponds to the tangency of the primary-beam axis with the (111) planes on the entrance face of the crystal. The color of a point corresponds to the number of protons, the color scale is shown on the right-hand side from the plot. Two effects are clearly seen in the plot, which cause particles to deviate oppositely with respect to the initial direction. The right and left spots are easily identified as the regions of the channeling effect and the volume reflection effect, respectively. The lower and upper spots correspond to the primary beam passing through the non-oriented crystal.

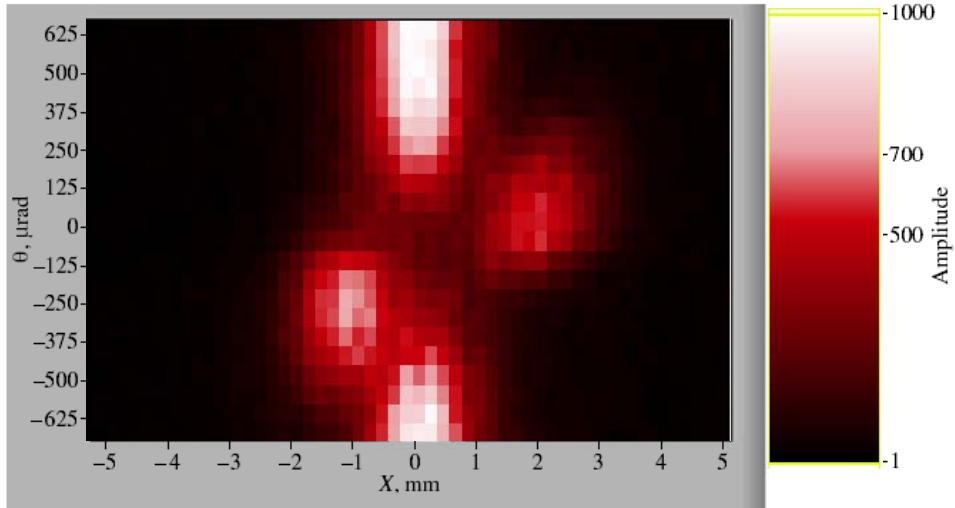


Fig. 8. Beam profile vs the angular position of the crystal as measured using the parallel plate position sensitive gas counter

Figures 9 and 10 show the profiles of the beam passed through the crystal in the angular positions corresponding to the centers of the channeling and volume reflection regions measured with the scintillation detector. The dashed line presents the beam profile corresponding to the non-oriented crystal.

From fitting of the peaks, the probability of the volume reflection equals to 0.71 ± 0.03 that is higher than probability of the channeling equal to 0.63 ± 0.03 . The deflection angle of protons reflected inside the crystal is equal to 1.39 ± 0.04 in terms of the critical angle for channeling. The width of the reflected peak is equal to 1.76 ± 0.04 in the same units.

The protons that are not involved in channeling undergo volume reflection and are deflected by an angle of 1.01 ± 0.05 in terms of the critical angle for channeling, and the width of the reflected peak is equal to 1.94 ± 0.08 in the same units.

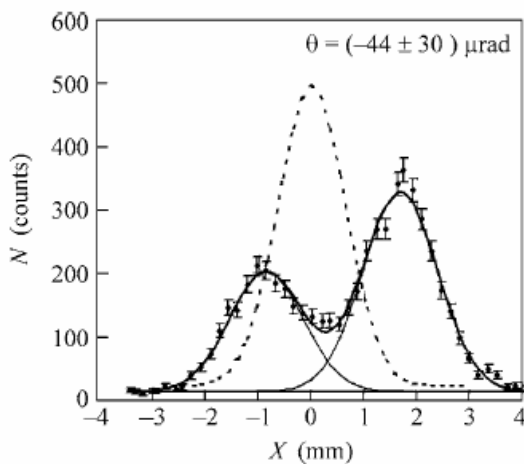


Fig. 9. Beam profile in the angular position of the crystal that corresponds to the maximum channeling as measured by means of the scintillation detector. The collection time at each point is equal to 10 s

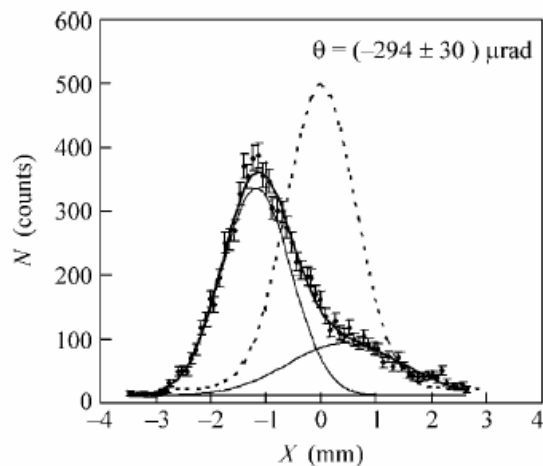


Fig. 10. Beam profile in the angular position of the crystal that corresponds to the maximum volume reflection as measured by means of the scintillation detector. The collection time at each point is equal to 10 s

5. Study of volume reflection effect in bent silicon crystals with 400 GeV proton beam at CERN

The experiment [6] was carried out with a 400 GeV proton beam from the CERN Super Proton Synchrotron H8 external line, which had a low divergence and an intensity near 10^4 particles per second. An experimental layout is shown in Fig. 11. It consisted of a high precision goniometer (G), where the crystals under investigation were mounted, and of various detectors to track particles. They were positioned along the beam line in the vicinity of the crystal and in an experimental area at about 70 m downstream.

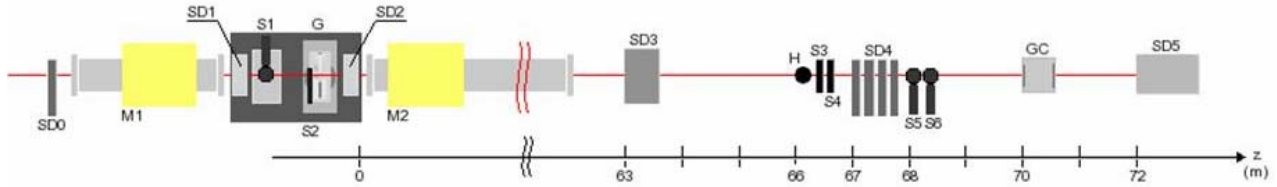


Fig. 11. Sketch of the H8-RD22 experimental setup. M1 and M2 are two bending magnets, part of the H8 beam transport line with no specific function for this experiment. See the text for more details

For the experiment, several quasi-mosaic and strip silicon crystals were prepared. In fact, the results of the measurements with all these crystals turned out to be very similar. Below a result from one of the strip crystals is presented. This crystal had (110) channeling planes bent (due to anticlastic effect) at an angle of $162 \mu\text{rad}$ along its 3 mm length in the beam direction. The multiple scattering angle of 400 GeV protons in this crystal was equal to $5.3 \mu\text{rad}$ and small with respect to the critical angle equal to $10.6 \mu\text{rad}$. The proton beam had a divergence of $8 \pm 1 \mu\text{rad}$, also smaller than the critical angle. The beam spot size was of about 1 mm close to the strip crystal thickness.

The goniometer consisted of three high precision motion units, two linear and one angular. With the linear motions, the crystals were positioned with respect to the beam center with an accuracy of several micrometers. With angular scans, the crystals were aligned with respect to the beam axis with an accuracy of $1.5 \mu\text{rad}$.

Six scintillator counters were used to determine the beam transverse offset with respect to the crystal (S1–S2), to provide the basic trigger signal for silicon detectors (S3–S4), and to measure the beam

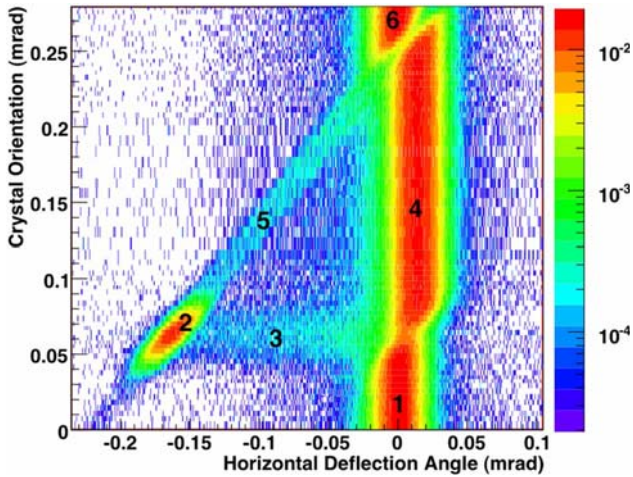


Fig. 12. Beam intensity recorded by the silicon microstrip detectors as a function of the horizontal deflection angle (X-axis) and the crystal orientation (Y-axis). Six regions can be distinguished: (1) and (6) non-channeling mode; (2) channeling; (3) dechanneling; (4) volume reflection; (5) volume capture. The wider angular acceptance of volume reflection compared to channeling is clearly visible in the figure

divergence and the beam profile (S5–S6). A scintillation hodoscope (H) and a position-sensitive gas chamber (GC) were operated in self-triggering mode for a fast prealignment of the crystal. High statistical runs were taken instead with a set of silicon microstrip detectors (SD n) of spatial resolution in the range 10–30 μm .

Figure 12 shows a summary plot of a scan performed with the crystal. A deflection angle of the channeled beam is equal to $165 \pm 2 \mu\text{rad}$ in agreement with the value of the bending angle of the crystal. An efficiency of the channeling is about 55%. A deflection angle of the volume reflected beam is equal to $13.9 \pm 0.2_{\text{stat}} \pm 1.5_{\text{syst}} \mu\text{rad}$, which is in agreement with the theory predictions. The volume reflection efficiency has been estimated to exceed 95%. This high efficiency is by far greater than the maximal theoretical single-pass efficiency for channeling.

6. Observation of double volume reflection of proton beam by a sequence of two bent crystals

Using the beam and setup described in previous section we have carried out an experiment on double volume reflection in two quasi-mosaic crystals [7]. Experimental layout is shown schematically in Fig. 13.

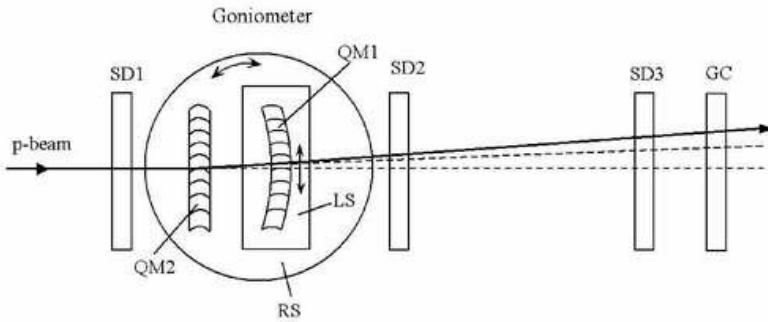


Fig. 13. Schematic top view of the experimental layout in the horizontal plane. QM1 and QM2 are two quasi-mosaic crystals installed on the rotational stage RS of the goniometer. The QM1 crystal is placed on the additional linear stage LS that allows to align QM1 with QM2. SD1, SD2, SD3 are silicon microstrip detectors, GC is a position-sensitive gas chamber. The lines represent the trajectories of the protons after the crystals, the unperturbed beam (lower dashed), the beam reflected by the first crystal only (upper dashed), and the double-reflected beam (solid)

Two silicon plates QM1 and QM2 with the (111) atomic planes bent of $\sim 70 \mu\text{rad}$ along the plate thickness of $\sim 0.8 \text{ mm}$ were installed on a goniometer. The (111) planes of QM1 plate were fan-shaped that made possible to align them with respect to the QM2 plate within the proton beam spot using the transverse linear motion of the QM1 support.

In Fig. 14 the angular scans performed before (a) and after (b) the fine relative alignment of the two crystals are shown. The channeling peaks for both QM2 and QM1 crystals are visible as the two isolated spots at negative values of the beam deflection angles in Fig. 14a. This scan was obtained before the alignment and, therefore, the two peaks appear at different angular positions of the goniometer.

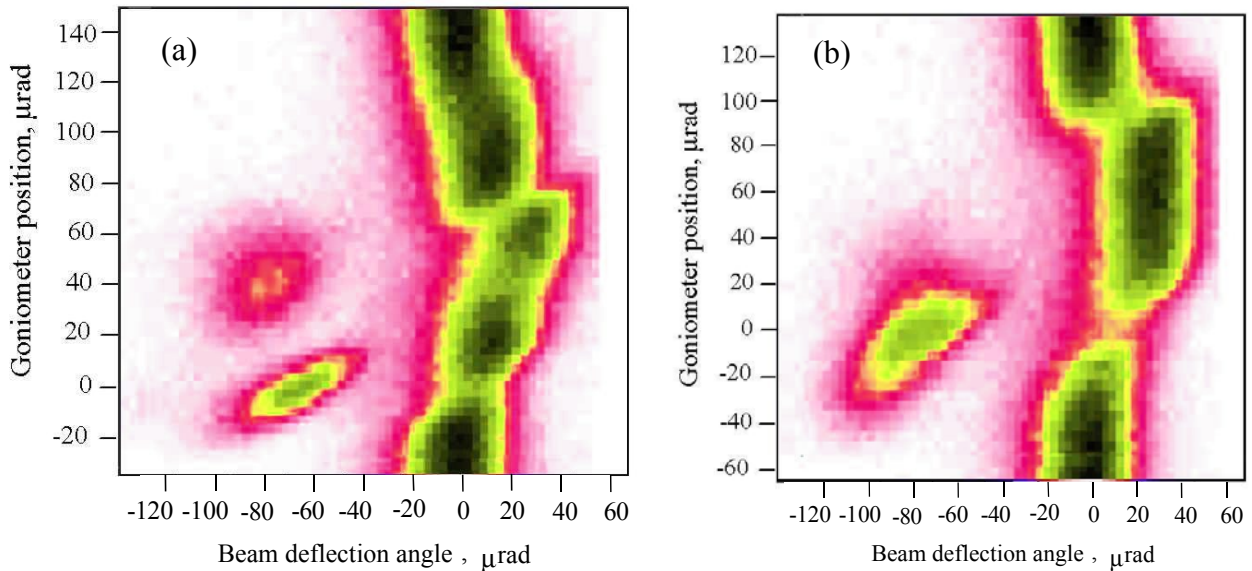


Fig. 14. Angular scans performed before (a) and after (b) the fine alignment of the crystals. On the Y-axis the angular position of the goniometer is shown while on the X-axis the beam deflection angle of the particle measured with the GC detector is reported. The origin of the X-axis corresponds to the direction of the incident beam. The origin of the Y-axis corresponds to the angular position of the goniometer when the channeling effect in QM2 crystal is maximal. In (a) both channeling peaks due to QM1 and QM2 are visible. In (b) the two channeling peaks coincide at about the same goniometer angle and are followed by the double reflection. The color scale indicates the beam intensity at a given deflection angle for various angular positions of the goniometer

The mean deflection angles of the channeled protons are measured with the SD2 and SD3 detectors to be $68.6 \pm 0.9 \mu\text{rad}$ and $78.1 \pm 4.8 \mu\text{rad}$ for the QM2 and QM1 crystals, respectively: they are equal to the bending angles of the (111) atomic planes in the crystals. The region of the scan with the proton beam

deflected to the opposite direction with respect to the channeled protons is due to the volume reflection effect. The deflection angle and efficiency of a single reflection are found to be $11.70 \pm 0.51 \mu\text{rad}$ and $(98.27 \pm 0.50)\%$ for QM2 and $11.90 \pm 0.59 \mu\text{rad}$ and $(97.80 \pm 0.64)\%$ for QM1, respectively.

The volume reflection regions corresponding to the QM2 and QM1 crystals in Fig. 14a are partly superimposed resulting in the deflection of the proton beam at larger angles than in the case of a single reflection. The angle and efficiency of double reflection were accurately measured with finally aligned crystals, the result is shown in Fig. 14b.

Figure 15 shows the beam profiles for three different cases corresponding to amorphous scattering, single, or double reflections of protons in the crystals. The deflection angle of the double reflected beam is found to be equal to $23.23 \pm 0.18_{\text{stat}} \pm 0.09_{\text{syst}} \mu\text{rad}$, that is twice larger than in the single reflection. The efficiency of the double reflection is equal to $(96.73 \pm 0.38_{\text{stat}} \pm 0.50_{\text{syst}})\%$.

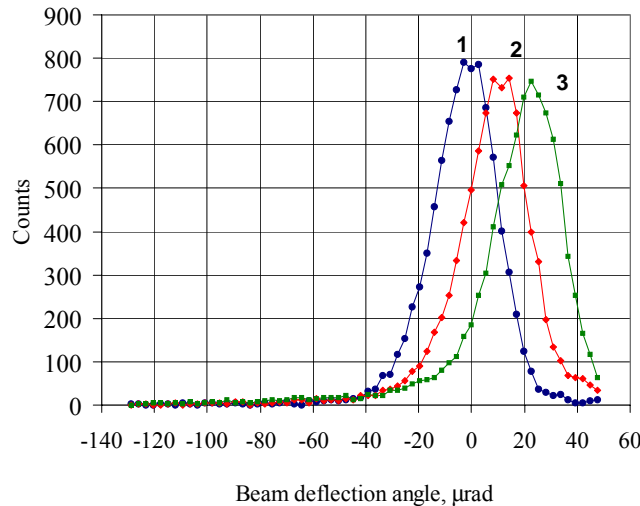


Fig. 15. The beam profiles corresponding to amorphous scattering of protons in both crystals (1), the reflection case in one of the crystal (2) and in both crystals – double reflection (3)

Thus, the experiment demonstrated a feasibility of multiple volume reflections in a sequence of short bent crystals with high efficiency and with beam deflection angle proportional to the number of reflections. This result opens new ways to develop crystal optics for the manipulation of high-energy charged particle beams.

7. Conclusion

In conclusion, the volume reflection exhibits high performance compared to channeling in terms of efficiency and angular acceptance, sheds new insight into the physics of interaction of charged particles with crystals, and suggests new applications in the next generation of experiments in both accelerators and high-energy physics.

References

1. Yu.M. Ivanov, A.A. Petrunin and V.V. Skorobogatov, Pis'ma v ZhETF **81**, 129 (2005) [JETP Lett. **81**, 99 (2005)].
2. Yu.M. Ivanov, A.A. Petrunin, V.V. Skorobogatov *et al.*, Preprint PNPI-2649, Gatchina, 2005. 22 p.
3. Yu.M. Ivanov, A.A. Petrunin and V.V. Skorobogatov *et al.*, Phys. Rev. Lett. **97**, 144801 (2006).
4. Yu.M. Ivanov, N.F. Bondar, Yu.A. Gavrikov *et al.*, Preprint PNPI-2687, Gatchina, 2006. 22 p.
5. Yu.M. Ivanov, N.F. Bondar, Yu.A. Gavrikov *et al.*, Pis'ma v ZhETF **84**, 445 (2006) [JETP Lett. **84**, 372 (2006)].
6. W. Scandale, D.A. Still, A. Carnera *et al.*, Phys. Rev. Lett. **98**, 154801 (2007).
7. W. Scandale, A. Carnera, G. Della Mea *et al.*, submitted to Phys. Lett. B (2007).